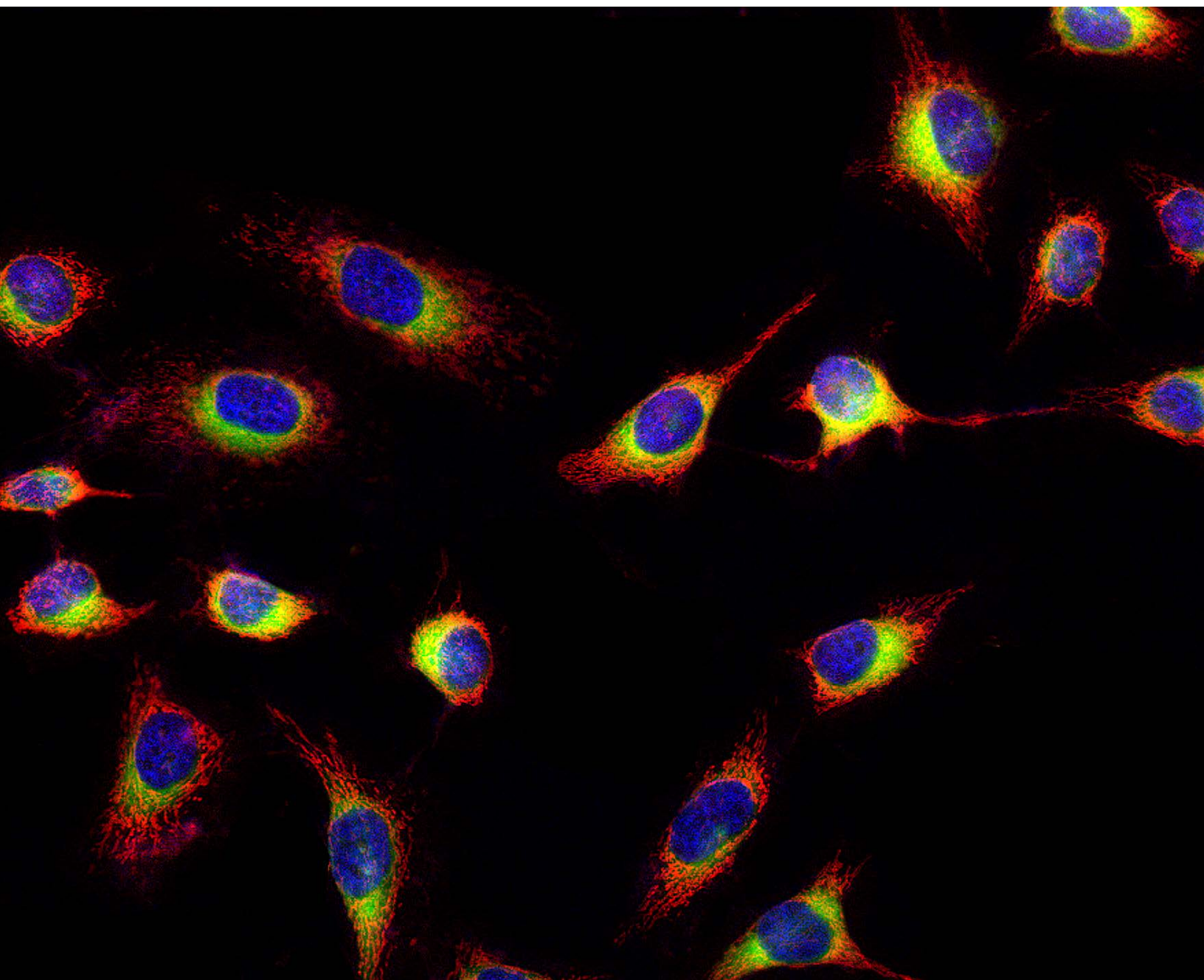


AssayWise Letters

2018 • Volume 7 • Issue 1



Novel Products & Tools

Mitochondria-Selective Tools

Featured Product

Phalloidin-iFluor™ Conjugates

Table of Contents

Product Spotlight	1
Luciferins	1
Allophycocyanin.....	1
ReadiUse™ TCEP Removal Buffer.....	1
A Comprehensive Suite of Online Tools	2
Regression Analysis	2
Spectral Data	4
Protein Calculators	4
Featured Products.....	6
Selective Probes for Studying Mitochondrial Functionality	6
A Superior Direct Method for the Quantitative Analysis of DNA Fragments in Late-Stage Apoptosis	11
Product Reviews	14
An Introduction to Lysyl Oxidase and Its Quantification	14
Fluorescent Phalloidin: A Practical Stain for Visualizing Actin Filaments	17

Trademarks of AAT Bioquest

AAT Bioquest®
 Amplite™
 Cell Meter™
 Cell Navigator™
 iFluor™
 JC-10™
 Nuclear Blue™
 MitoLite™
 MitoROS™
 Nuclear Blue™
 Nuclear Green™
 ReadiUse™
 Screen Quest™
 Tunnelyte™

Trademarks of Other Companies

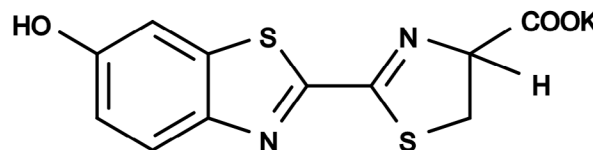
Alexa Fluor® (Thermo Fisher)
 Click-iT™ (Thermo Fisher)
 Cy3® & Cy5® (GE Healthcare)
 DeadEnd™ (Promega)

On the cover:

Mitochondria of live HeLa cells were labeled with mitochondrial dye MitoLite™ Deep Red FX660 (Cat# 22678). Green-fluorescent Cell Navigator™ Live Cell Endoplasmic Reticulum Staining Kit (Cat# 22635) was used to stain ER. The cells were counterstained with blue-fluorescent Hoechst 33342 (Cat# 17530) to image nuclei.

Luciferins

Luciferins are a powerful and versatile class of chemiluminescent substrates that can emit light upon oxidation catalyzed by various types of luciferases. This bioluminescent system is used in various applications and is known for its high sensitivity, background-free luminescence, speed, and affordability. The luciferin-luciferase reaction is often utilized for detecting low level gene expression and cellular ATP activity, for in vivo imaging and in various reporter assays. AAT Bioquest provides an array of luciferase substrates and reporter gene assays optimized to yield consistent results with high sensitivity over a wide dynamic range.



The chemical structure of D-Luciferin, potassium salt (Cat# 12507).

Allophycocyanin

Allophycocyanin (APC) is a phycobiliprotein that exhibits a far-red fluorescence with a high absorptivity and quantum efficiency. Its high water solubility, large Stokes shift and quench-resistant properties make it effective in fluorescence-based applications (primarily in flow cytometry, immunoassays, and FRET/tandem dyes). AAT Bioquest offers a broad range of APC products including secondary antibody and streptavidin conjugates, tandem dyes, and APC-labeling kits.

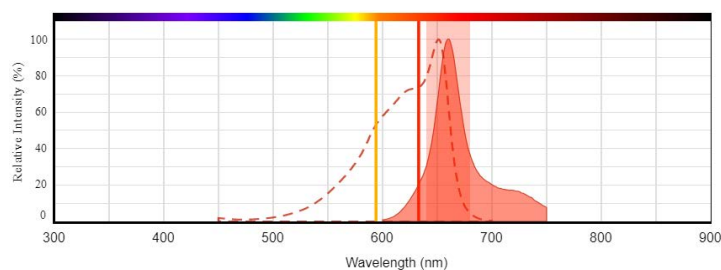
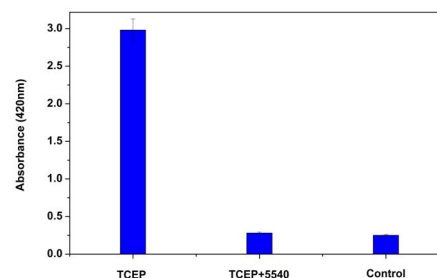


Image courtesy AAT Bioquest, Inc. (<https://www.aatbio.com>)

Absorption and emission spectrum of APC (Cat#2554). Excitations at 594 nm (Orange laser line) and 633 nm (Red laser line). APC read with emission filter Cy5* (Red band).

ReadiUse™ TCEP Removal Buffer

Tris(2-carboxyethyl)phosphine (TCEP) is a potent disulfide reducing agent frequently utilized in biochemistry and molecular biology applications. TCEP is used as a reducing agent to break disulfide bonds between proteins for gel electrophoresis. It is used in the tissue homogenization process for RNA isolation, and in site-specific conjugation of protein or antibody cysteine residues with maleimide derivative labels (e.g., iFluor™ 488 maleimide). Due to its potent reactivity, the removal of TCEP is essential in most downstream applications. AAT Bioquest's ReadiUse™ TCEP removal buffer effectively eliminates residual TCEP in less than one hour with a single mixing step.



ReadiUse™ TCEP removal buffer (Cat #5540). TCEP was treated with/without ReadiUse™ TCEP removal buffer for 10 minutes. Mixture was then incubated with Ellman's reagent for 30 minutes.

A Comprehensive Suite of Online Tools

AAT Bioquest offers a suite of online tools to aid researchers in post-experimental data analysis. These tools are free to use for all researchers and complement our extensive catalog of assays and kits. Here, we provide a rough description of these web-tools, which can be broken down into three main categories: regression analysis, spectral analysis and protein analysis.

As always, all tools and related products can be found online at aatbio.com.

Regression analysis

Regression analysis is a statistical technique for modeling data and analyzing the relationship between variables (e.g. independent and dependent). This relationship is expressed as a “best-fit” line, or an equation that best represents the experimental data set. Depending on the type of experiment and data, different regression models can be chosen. For biochemical assays, such as ELISAs, regression analysis typically consists of one of three different types: linear analysis, logarithmic analysis and four parameter logistical analysis.

Linear analysis, or linear regression, is used when there is a simple scalar relationship between the independent variable (x) and the dependent variable (y). The equation for linear regression is that of a straight line, which follows the form:

$$y = mx + b$$

y is the dependent variable (i.e. response)
x is the independent variable (i.e. treatment)
m is the scalar or slope
b is the y-intercept (i.e. y when x = 0)

Linear regression typically uses a least squares method to determine the slope and intercept for a given dataset. The degree of fitness for a given regression line is expressed as R-squared (R²), where R² > 0.95 or R² > 0.98 is considered “good”.

Logarithmic analysis (also known as log-log analysis or power law analysis) is used when the relationship between the independent variable (x) and the dependent variable (y) is exponential rather than linear. This type of analysis is often used when modeling standard curves for experiments. This is because standard curves are

generated in a non-linear fashion (i.e. using serial dilutions). While the relationship between the independent and dependent variables is exponential, the graphed line is still linear (i.e. straight line) if both the x-axis and y-axis are set to logarithmic scale. In Microsoft Excel, this type of regression is called “Power Regression”. Logarithmic analysis generates an equation of the form:

$$y = ax^k$$

y is the dependent variable (i.e. response)
x is the independent variable (i.e. treatment)
a is the scalar for the function
k is the exponent denoting the proportionality between x and y

Like linear analysis, logarithmic analysis can utilize an R-squared value to represent the fitness of a given “best-fit” line, where again R² > 0.95 or R² > 0.98 is considered “good”.

Concentration	Response 1
3	11400
1	3800
0.333	1350
0.111	500
0.037	200
0.012	120
0	50

Graph Options	
X-Axis Label	Concentration
Y-Axis Label	Response 1
Title	(Optional)
Display error bars	<input checked="" type="checkbox"/>

Calculate Regression

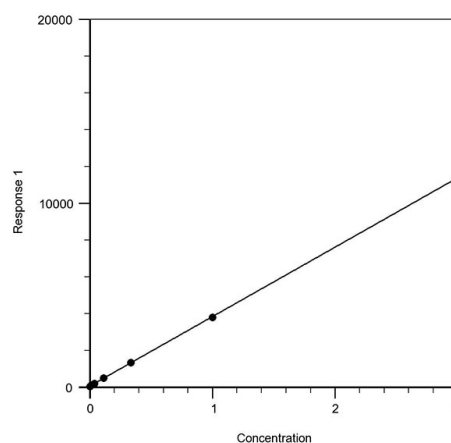


Figure 1.1. The linear regression graph of Amplitude™ Fluorimetric Peroxidase (HRP) Assay Kit (Cat# 11552) using Linear Regression Calculator.

Data 1	
Equation	y = 3775.01 x + 65.11
R-squared (R ²)	1
Enter X below to calculate Y	Enter Y below to calculate X

Figure 1.2. The linear regression equation and results of Amplitude™ Fluorimetric Peroxidase (HRP) Assay Kit (Cat# 11552) using Linear Regression Calculator.

Lastly, we have a tool for four parameter logistical (4PL) analysis, which is a type of logistic regression (not to be confused with logarithmic). Four parameter logistical plots are often expressed as sigmoidal, or "s"-shaped, curves. This type of modeling is useful when a data set approaches limits on either end (i.e. the minimum and maximum) while having a non-linear function in the middle. This type of modeling is commonly used to analyze inhibition assays (e.g. drug potency experiments) and is particularly useful for determining various half-max response values such as IC₅₀, EC₅₀, LD₅₀ and LC₅₀. A term often related to this type of regression is probit, or logit, models, which can be determined using similar methodology. In 4PL analysis, the equation takes the form:

$$y = A + \frac{B - A}{1 + \left(\frac{x}{C}\right)^D}$$

y is the dependent variable (i.e. response)
x is the independent variable (i.e. treatment)
A is the lower limit of the dataset (i.e. minimum)
B is the upper limit of the dataset (i.e. maximum)
C is the x value of the inflection point (i.e. IC₅₀, EC₅₀, LD₅₀ or LC₅₀)
D is the slope at the inflection point (i.e. Hill slope)

A few important things should be kept in mind when using 4PL analysis.

1. The inflection point is the point at which the first derivative of the function changes signs (either from positive to negative or negative to positive). It is also the point wherein the response value is halfway between the minimum and the maximum limits of the function. The actual slope at the inflection point, known as the Hill slope, will be positive in an overall downward curve (i.e. inhibition assay) or negative in an overall upward curve (i.e. dose-response assay).
2. The curve of the function will be mirrored symmetrically before and after the inflection point. If the data set is not symmetrical around the inflection point, then five parameter logistical (5PL) analysis must be used. This is also called Richards' curve or generalized logistic function.

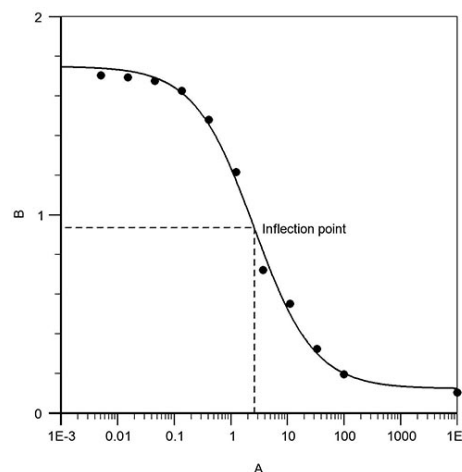
3. 4PL analysis is not well represented by an R-squared value. This is because R-squared values are suitable for linear models due to the way they are calculated and have little meaning when applied to non-linear models. That is, a high R-squared value does not necessarily equate to a good best-fit line in non-linear models.
4. The inflection point generated by the 4PL model is typically thought of as the relative inflection point. This means that the response value at the inflection point (i.e. the half-max response) is calculated such that:

$$\text{half max} = \frac{\text{max} - \text{min}}{2}$$

The other way to interpret half-max response is to understand it as the absolute inflection point. This interpretation is represented by the equation:

$$\text{half max} = \frac{\text{max} - 0}{2}$$

Care should be taken in interpreting our online calculator results as the half-max response values given are relative half-max response values and not absolute half-max response values.



Inflection point = 2.600

$$y = 0.123 + \frac{(1.749 - 0.123)}{1 + \left(\frac{x}{2.600}\right)^{0.821}}$$

Enter X below to calculate Y	Enter Y below to calculate X

Figure 1.3. The 4PL equation & results of Screen Quest™ Colorimetric ELISA cAMP Assay Kit (Cat# 36370) using Four Parameter Logistic (4PL) Curve Calculator.

Spectral Data

AAT Bioquest offers a Spectrum Viewer tool that allows users to display and compare spectral curves for an extensive library of fluorophores. This tool is particularly useful during the initial planning phases of an experiment as it allows researchers to find fluorophores which match their application as well as their instrumentation. For example, researchers can display fluorophores with excitation sources (e.g. lasers) and filter sets to determine if a particular fluorophore is suitable with a given instrument setup. Researchers can also use the Spectrum Viewer tool to find alternatives for fluorophores. This is easily accomplished through filtering of fluorophores by excitation, emission and Stokes' shift properties. Finally, our Spectrum Viewer tool is uniquely able to export a given setup as either an image or a sharable link. This allows for easy and seamless collaboration amongst researchers.

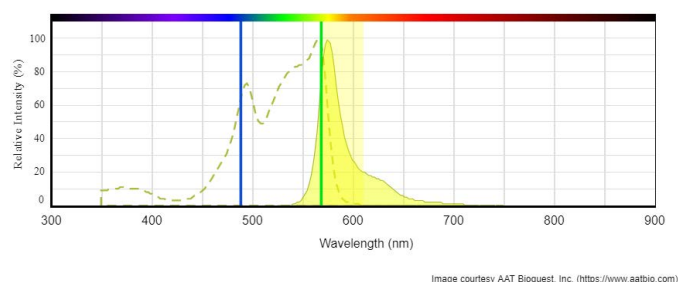


Figure 1.4. Absorption and emission spectrum of PE (Cat# 2556). Excitations at 488 nm (Blue laser line) and 568 nm (Green laser line). PE read with emission filter Cy3[®]/TRITC (Yellow band).

For more comprehensive experimental planning, the spectrum viewer tool can also be combined with our Extinction Coefficient Finder tool. This tool is a queryable database of extinction coefficients for all common fluorophores. Researchers are typically interested in this value as it provides a rough estimate of a fluorophore's brightness. It is important to note, of course, that the actual brightness of a fluorophore and its performance in a particular application greatly varies depending on the actual experimental conditions. But as a first-pass metric, the extinction coefficient is a valid quantity for narrowing down potentially desirable fluorophore.

Protein Calculators

AAT Bioquest offers two extremely useful tools for protein analysis.

The first tool is our protein concentration calculator. In order to use

this tool, a user simply has to select their protein and enter the OD at max absorbance (λ_{max}). For most proteins and antibodies, λ_{max} is at 280 nm. Thus, users simply need to enter the absorbance value at 280 nm as measured by a spectrophotometer. Optionally, users may also choose to include a dilution factor and an adjusted path length in their calculations. The path length of a standard quartz cuvette is 1 cm (default).

In choosing the protein, users have the option of picking from a pre-selected set of common proteins such as IgG and BSA. Alternatively, users can enter the amino acid sequence of a custom protein. The UniProt ID can also be used. If a custom sequence is used, the calculator will also supply the molecular weight and the extinction coefficient of the sequence for use in calculations.

This calculator works by utilizing the well-established Beer-Lambert law, which defines the relationship between concentration and absorbance of a given substance. The equation can be simplified to the following form:

$$A = a_{\lambda} \times b \times c$$

A is the absorbance
 a_{λ} is the molar absorption coefficient or extinction coefficient
 b is the path length
 c is the concentration

Re-written for concentration, the equation is as follows:

$$C = A/a_{\lambda}b$$

The equation can also be adjusted for a dilution factor and for conversion between molarity (M) and mass/volume (g/L). The revised equation is as follows:

$$C = A/a_{\lambda}b \times \text{MW} \times \text{DF}$$

MW is the molecular weight
 DF is the dilution factor

A second tool for protein analysis is our degree of labeling (DOL) calculator. The DOL (sometimes called degree of substitution, DOS) is the average ratio of labels bound per target macromolecule (e.g. protein). This value is especially important when determining the success of bioconjugation reactions. A DOL that is too low often

represents low conjugation efficiency. Additionally, if the DOL is too low, the signal generated from the bioconjugate (e.g. colorimetric or fluorimetric) may be too weak to detect. On the other hand, if the DOL is too high, the conjugation product may suffer steric issues (such as blocking of active sites) or poor solubility in aqueous solutions.

For antibody conjugates, the optimal DOL usually falls in-between two to ten, that is, two to ten labels per antibody. However, the exact DOL should always be determined experimentally depending on the label-antibody pair. An alternative to testing the DOL is to use a pre-tested conjugation system, such as our antibody labeling kits. These kits provide optimized labeling ratios for precision biological applications.

The DOL is calculated by essentially applying the Beer-Lambert law twice, once for the label and once for the target, and then dividing the two resulting concentrations. Two important things must be kept in mind, however, when calculating the DOL.

1. A correction factor is required (CF_{280}) for every given label-target pair to account for any spectral overlaps. This value must be experimentally determined or, in the case of our antibody labeling kits, provided in the product specifications

2. The bioconjugate must be purified before using a spectrophotometer to measure the absorbances. If not, excess label or target substrates will bias the concentration values.

AAT Bioquest's Online Interactive Tools:

- Buffer Preparation and Recipes
- Degree of Labeling Calculator
- DNA Molecular Weight Calculator
- Extinction Coefficient Finder
- EC_{50} Calculator
- ED_{50} Calculator
- IC_{50} Calculator
- LC_{50} Calculator
- LD_{50} Calculator
- Interactive Spectrum Viewer
- Peptide and Protein Molecular Weight Calculator
- 4PL Calculator
- Protein Concentration Calculator
- RNA Molecular Weight Calculator
- Serial Dilution Calculator

The screenshot shows the AAT Bioquest website with the navigation bar at the top. The main content area is titled "Degree of Labeling (DOL) Calculator". Below the title, there is a paragraph explaining the DOL parameter. Further down, there is a section titled "How to use this tool:" with three numbered steps. To the right of the steps, there is a form with the following fields: "Select target:" with a dropdown menu, "Select label:" with a dropdown menu, "Absorbance of target:" with a text input field, and "Absorbance of label:" with a text input field. At the bottom of the form is a yellow "Calculate" button.

Home > Tools > Degree of Labeling Calculator

Degree of Labeling (DOL) Calculator

The Degree of Labeling (DOL), sometimes called Degree of Substitution (DOS), is a particularly useful parameter for characterizing and optimizing bioconjugates, such as fluorophore-labeled proteins. It is expressed as a molar ratio in the form of label/protein. In general, conjugates with lower DOL values tend to have weaker fluorescence intensities. However, bioconjugates with very high DOL values (e.g. DOL > 6) may also experience reduced fluorescence. This often occurs as a result of self-quenching from the fluorophore. An accurate DOL value will allow a researcher to find the most optimal bioconjugation ratio for a given labeling as well as ensure reproducibility in conjugation results.

For antibodies, the optimal DOL usually falls between 2 to 10. A more precise value, however, will largely depend on the properties of the label and protein. This means that for many bioconjugations, the optimal DOL must be experimentally determined, often through several small-batch labelings. For AAT Bioquest's [antibody labeling kits](#), the optimal DOL and reagent quantities have already been tested. For other bioconjugates, the tool below can be used to calculate the degree of labeling.

How to use this tool:

1. Select a target from the drop down menu. After selecting a target, a list of labels will become available.
2. Select a label from the drop down menu.
3. Enter the maximum absorbance values for both the target and label. Note that the provided wavelengths are typical maximal wavelengths for the given compounds. However, for optimal results, use the maximal absorbances as determined by actual spectrophotometer readings.

Select target:

Select label:

Absorbance of target:

Absorbance of label:

Figure 1.5. The Degree of Labeling (DOL) Calculator.

Selective Probes for Studying Mitochondrial Functionality

It is indisputable that mitochondria are the primary producers of cellular energy via oxidative phosphorylation and lipid oxidation. In addition to their role as the cell's powerhouse, mitochondria have a key role in other vital cell physiological and pathological processes. For example, mitochondria play a role in regulating intrinsic pathways of apoptosis. They also contribute to buffering and shaping cytosolic calcium, and are potent producers of cellular reactive oxygen species (ROS), such as superoxide ($\cdot\text{O}_2^-$). Furthermore, mitochondrial dysfunction is a characteristic of many chronic diseases, including neurodegenerative and cardiovascular diseases, and chronic fatigue.

AAT Bioquest offers a broad selection of tools designed to investigate mitochondrial morphology and functionality, and ROS imaging. The following discussion highlights assay reagents and kits optimized for mitochondrial ROS imaging, as well as, exploring a convenient method for improving Rhod-2 sensitivity at detecting mitochondrial calcium. For a detailed overview of the various tools we provide to monitor mitochondrial morphology and functionality refer to the Table 1 & 2.

Mitochondria ROS Imaging

A byproduct of mitochondrial oxidative phosphorylation is ROS. These chemically reactive, oxygen-containing species are released into the cytoplasm to promote redox signaling. However, an improper balance of ROS production-detoxification leads to oxidative stress (ROS overproduction), which is characterized by the potentially damaging levels of intracellular ROS. Because ROS overproduction is detrimental to mitochondria it must be neutralized in order maintain normal cellular homeostasis. Failure to do so will result in damage to the organelle's lipids, proteins and DNA, and can induce cell damaging activities such as the induction of the mitochondrial permeability transition pore (mPTP). Opening of the mPTP channel is accompanied by an increase in the inner membrane permeability, the dissipation of the mitochondrial membrane potential, and a decrease in ATP production. The changes induced by the opening of mPTP can induce cell death.

Consequently, all of these different aspects of mitochondrial ROS have also been implicated in various pathologies including isch-

emia reperfusion injury, myocardial infarction, and chronic disorders (e.g., neurodegenerative disease, or type-2 diabetes). As such, the detection and quantification of mitochondrial ROS is important to understanding proper cellular redox regulation and the impact of its dysregulation on various cellular pathways and pathologies.

Superoxide Radical

Mitochondria are potent producers of cellular superoxide ($\cdot\text{O}_2^-$), a by-product of mitochondrial respiration (most notably by Complex I and Complex III). Superoxide is the predominant ROS in mitochondria. Superoxide, at low to moderate levels, is critical for the proper regulation of many essential cellular processes including gene expression and signal transduction. However, studies have shown mice deficient for mitochondrial superoxide dismutase (enzyme that neutralizes superoxide radicals) die due to neurodegeneration, cardiomyopathy and lactic acidosis (pathologies commonly correlated with elevated superoxide levels) (Muller et al. 2007). Therefore, investigating mitochondrial superoxide (exogenous or endogenous) levels are of great interest to study these medically relevant pathologies.

Cell Meter™ Fluorimetric Mitochondrial Superoxide Activity Kit

MitoROS™ 580 shares similar characteristics with dihydroethidium (a widely utilized superoxide indicator) and Invitrogen's MitoSOX™ Red. Therefore, experiments utilizing dihydroethidium or MitoSOX™ Red can be replaced with MitoROS™ 580 without any sacrifice in assay sensitivity. In fact, MitoROS™ 580 is less likely to be oxidized by other reactive oxygen species and reactive nitrogen species (Figure 2.1). MitoROS™ 520 and MitoROS™ 580 are two unique superoxide indicators and are the central components of our Cell Meter™ Fluorimetric Mitochondrial Superoxide activity assays. The cationic property of both probes facilitates their diffusion across the cytoplasmic and mitochondrial membranes as well as promotes their potential driven uptake within the mitochondria via the mitochondrial membrane potential. Similar to other commercially available $\cdot\text{O}_2^-$ indicators, MitoROS™ 520 and MitoROS™ 580 probes are activated through oxidation by superoxide. Activated MitoROS™ 520 and MitoROS™ 580 probes then intercalate with DNA, which is essential for the generation of their strong fluorescence signals.

Upon excitation, MitoROS™ 520 generates a green fluorescence while MitoROS™ 580 fluoresces red.

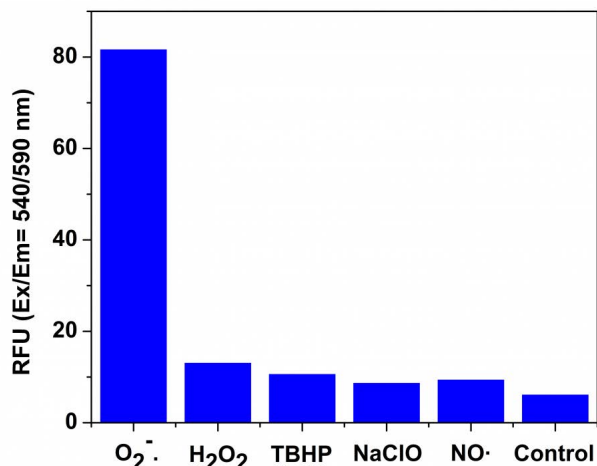


Figure 2.1. Fluorescence response of MitoROS™ 580 (10 μM, Cat# 16052) to different reactive oxygen species (ROS) and reactive nitrogen species (RNS). The fluorescence intensities were monitored at Ex/Em = 540/590 nm.

MitoROS™ 520 is unique in that it generates a strong green fluorescence when it is oxidized by superoxide and binds to DNA (Figure 2.2). Utilization of the green spectrum creates enough spectral separation from other red ROS indicators, such as MitoROS™ OH 580 (a hydroxyl radical indicator) making it suitable for the simultaneous monitoring of superoxide and hydroxyl radical levels. Or one can investigate mitochondrial calcium uptake and ROS production using MitoROS™ 520 and Rhod-2, a red calcium indicator.

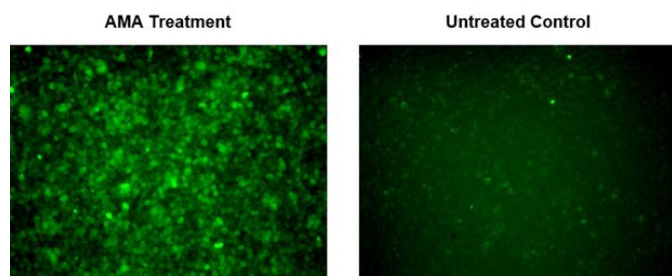


Figure 2.2. Fluorescence images of superoxide measurement in macrophage cells using Cell Meter™ Fluorimetric Mitochondrial Superoxide Activity Assay Kit (Cat#16060). RAW 264.7 cells at 100,000 cells/well/100 μL were seeded overnight in a 96-well black wall/clear bottom plate. AMA Treatment: Cells were treated with 5 μM Antimycin A (AMA) at 37 °C for 2 hours, then incubated with MitoROS™ 520 for 1 hour. Untreated Control: RAW 264.7 cells were incubated with MitoROS™ 520 at 37 °C for 1 hour without AMA treatment. The fluorescence signal was measured using fluorescence microscope with a FITC filter.

Hydroxyl Radical

The hydroxyl radical (•OH) is another byproduct of oxidative metabolism and is the most reactive ROS. Hydroxyl radicals can produce DNA damage and cause significant subcellular damage to organelles. Therefore, sensitive and selective detection of intracellular •OH

is vital to understanding cellular redox and the impact of hydroxyl radicals on dysregulation in cells. While a variety of •OH fluorogenic sensors are commercially available, many suffer from rapid photobleaching, short emission wavelengths, and non-selective reactions with other ROS species. All these factors have limited the applications in cells and tissues. To resolve these limitations, AAT Bioquest has dedicated extensive research and development in producing MitoROS™ OH580, a robust and sensitive •OH fluorogenic sensor.

Cell Meter™ Mitochondrial Hydroxyl Radical Detection Kit

MitoROS™ OH580 is the main component of our Cell Meter™ Mitochondrial Hydroxyl Radical Detection Kit. This novel fluorogenic indicator is cell-permeant and highly selective for hydroxyl radicals over other ROS, such as superoxide or hydrogen peroxide. MitoROS™ OH580's specific interaction with •OH greatly minimizes non-specific background fluorescence and significantly enhances intracellular •OH signals. Upon association with •OH, MitoROS™ OH580 exhibits a strong red fluorescence. This fluorescence signal can be monitored by fluorescence microscopy or measured using a fluorescence microplate reader at Ex/Em = 540/590 nm. MitoROS™ OH580's utilization of the red spectrum makes multiplexing possible with mitochondrial morphological probes of green fluorescence.

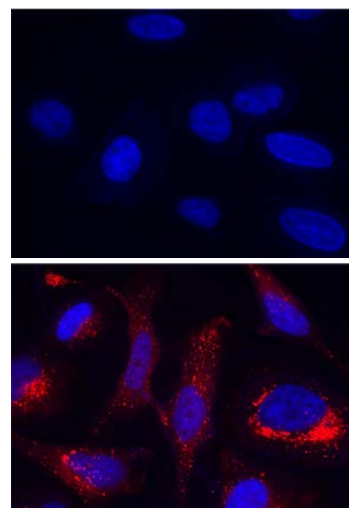


Figure 2.3. Fluorescence images of Hydroxyl radical measurement in HeLa cells using Cell Meter™ Mitochondrial Hydroxyl Radical Detection Kit (Cat#16055). Control (Top): HeLa cells were kept in 1X HBSS buffer without treatment. Cell nuclei were stained with Hoechst 33342 (Blue, Cat#17530). Fenton Reaction (Bottom): Cells were then treated with 10 μM CuCl₂ and 100 μM H₂O₂ in 1X HBSS buffer at 37 °C for 1 hour. After washing 3 times with HBBS, HeLa cells were measured using a fluorescence microscope with a TRITC filter set (Red).

Mitochondrial Calcium Imaging

Calcium uptake and efflux in mitochondria is important in regulating cytosolic calcium concentrations and metabolic

processes. Mitochondrion possess the ability to rapidly take up calcium, primarily through the mitochondrial calcium uniporter (MCU) located on the inner mitochondrial membrane. Calcium influx into the mitochondrial matrix is dependent upon the organelles electrochemical gradient for calcium. This gradient is established and maintained by mitochondrial respiration, while the mitochondrial sodium-calcium antiporter is responsible for sustaining a low resting intramitochondrial calcium concentration.

Intramitochondrial calcium plays an intimate role in regulating mitochondrial metabolism by targeting three key rate limiting dehydrogenases of the citric acid cycle (CAC). Calcium directly binds to the enzyme complexes and activates α -ketoglutarate and isocitrate dehydrogenases. Pyruvate dehydrogenase activation is mediated through a calcium-dependent dephosphorylation step. Calcium activation of these dehydrogenase enzymes in mitochondria leads to an increase in NADH and the production of ATP. Disruption of mitochondrial calcium uptake alters the spatiotemporal properties of cytosolic calcium signaling and suppresses mitochondrial metabolism, which leads to a decrease in ATP production. This type of disruption of mitochondrial calcium uptake has been found to cause diseases such as chronic fatigue.

Rhod-2: Mitochondrial Calcium Indicator

Rhod-2, AM can be used to measure changes in mitochondrial calcium inside cells. Rhod-2, AM is a rhodamine-based calcium indicator that is conjugated with AM esters to become cationic.

This is advantageous for two reasons: 1). the cationic charge on Rhod-2, AM promotes the potential driven accumulation of Rhod-2 within mitochondria via mitochondria membrane potential 2). AM esters facilitate the diffusion of Rhod-2 across the cytoplasmic membrane as well as the mitochondrial membrane. Once inside the mitochondria, non-specific intracellular esterases remove the AM groups, which traps Rhod-2 inside the mitochondria. Rhod-2 exhibits a significant increase in fluorescence intensity upon association with calcium ions.

Rhod-2 has a fluorescence excitation and emission maxima at 549 nm and 578 nm, respectively. This characteristically long-wavelength makes it suitable for cellular and tissue imaging which have relatively high autofluorescence. This is an advantage for detecting

calcium release generated by photoreceptors and photoactivatable chelators.

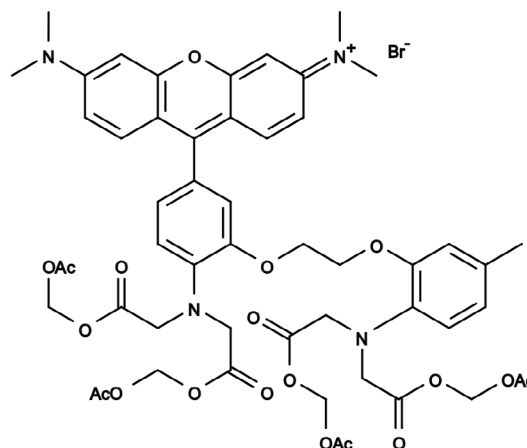


Figure 2.4. The chemical structure for Rhod-2, AM *UltraPure Grade* CAS#: 145037-81-6 (Cat# 21062).

One of the disadvantages of Rhod-2 AM is its susceptibility to background interference. Non-specific intracellular esterases are not unique to mitochondria and are present throughout the cytosol. When Rhod-2 AM is loaded into cells, the indicators can be activated and retained within the cytosol before it can be sequestered within mitochondria. A solution for improving Rhod-2 sensitivity is to reduce it to dihydrorhod-2 AM prior to use.

Improving Rhod-2 Sensitivity:

Method to Reduce Rhod-2 to Dihydrorhod-2

Reduction of Rhod-2 AM to dihydrorhod-2 AM enhances its mitochondrial localization and reduces background interference. This change improves sensitivity because it requires a two-part activation process. The non-fluorescent dihydrorhod-2 AM can only exhibit calcium-dependent fluorescence after oxidation and AM cleavage in the mitochondria. Residual dihydrorhod-2 retained in the cytosol, due to AM cleavage, cannot be taken up by the mitochondria for oxidation and will remain non-fluorescent even in the presence of cytosolic calcium. Reduction of Rhod-2 AM to dihydrorhod-2 AM can be readily achieved using the protocol below:

1. Dissolve 50 μ g of Rhod-2 AM in 100 μ L of anhydrous dimethylsulfoxide (DMSO).
2. Add a small excess (the smallest amount solid that can be practically transferred is sufficient enough) of solid sodium borohydride (NaBH_4).

- Incubate for 10 minutes or until the reaction mixture appears colorless.
- Use the reaction solution in DMSO (about 0.4 mM dihydorrhod-2 AM) directly for cell loading according to usual AM ester loading protocols.

**Note: Dihydorrhod-2 AM will spontaneously and rapidly revert to its oxidized form, this is indicated by reappearance of color in your stock solution. So, experiments using dihydorrhod-2 AM should be carried out immediately after preparation.*

Appendix: AAT Bioquest Mitochondrial Tools

The following tables provide a summary of the AAT Bioquest's mitochondrial tools and stains as well as their targets.

Table 1. AAT Bioquest Tools to Study Mitochondrial Functionality

Target	Tool	Cat#	Ex/Em (nm)	Application	Principle
Mitochondrial Calcium Flux	Rhod-2, AM	21060, 21062, 21063, 21064	549/578	Live Cells	Cationic calcium indicator. This unique property allows it to be sequestered in mitochondria via the $\Delta\Psi$ M. Cleavage by esterases activates rhod-2's calcium-dependent fluorescence. Upon excitation rhod-2 fluoresces red.
Mitochondrial Membrane Potential Probes	Rhodamine 123	22210	507/529	Live Cells	These cell-permeable, cationic probes localize in the mitochondria via the $\Delta\Psi$ M and are designed to quantify changes in $\Delta\Psi$ M. Mitochondria with decreased $\Delta\Psi$ M will fail to sequester probes. Upon excitation Rhodamine 123 will fluoresce green. TMRM and TMRE both will fluoresce red-orange.
	TMRM	22221	549/574		
	TMRE	22220	549/573		
	JC-1	22200	515/529	Live Cells	JC-1 is a cationic probe used to determine $\Delta\Psi$ M. It exhibits potential-dependent uptake by mitochondria which is represented by a fluorescence emission shift from green to red. At low concentrations, JC-1 exists as a monomer and when excited it fluoresces green. At higher concentrations, the dye forms 'J-aggregates' which fluoresces red.
	JC-10™	22204, 22800, 22801	510/525	Live Cells	JC-10™ is a superior alternative to JC-1. Its improved solubility and higher signal-to-noise ratio makes for a more convenient and robust assay. JC-10™'s potential-dependent spectroscopic properties are identical to JC-1.
Mitochondrial Oxidative Phosphorylation	MitoROS™ 580	10652	510/580	Live Cells	These probes passively permeate intact cells and sequester within the mitochondria. Probes are activated via oxidation by superoxide. Upon activation probes intercalate with DNA and fluoresce upon excitation. DNA binding is necessary for strong fluorescence signal.
		22970	540/590		
		22971	540/590		
	MitoROS™ 520	16060	509/534	Live Cells	Probe readily diffuses through intact cell membranes and selectively accumulates in mitochondria. It is oxidized by superoxide and when excited it generates a green fluorescence.
	MitoROS™ OH580	16055	576/598	Live Cells	Probe freely permeates live cells where it selectively targets free hydroxyl radicals. Oxidation by hydroxyl radicals activates the probe and when excited it generates a red fluorescence.

Table 2. AAT Bioquest Tools to Study Mitochondrial Morphology

Probe	Cat#	Ex/Em (nm)	Fixable	Application	Principle
MitoLite™ Blue FX490	22674	350/490	Yes	Live Cells	Cationic fluorogenic probe sequestered by functioning mitochondria via the mitochondrial membrane potential gradient ($\Delta\Psi$ M). MitoLite™ FX dyes retain fluorescent staining pattern after fixation and permeabilization.
MitoLite™ Green EX 488	22675	498/520	No		
MitoLite™ Green FM	22695	491/513	Yes		
MitoLite™ Orange EX405	22679	399/550	No		
MitoLite™ Orange FX570	22676	545/575	Yes		
MitoLite™ Red FX600	22677	575/600	Yes		
MitoLite™ Deep Red FX660	22678	640/659	Yes		
MitoLite™ NIR Red FX690	22690	660/692	Yes		

References

- Bowser, D N et al. "Role of Mitochondria in Calcium Regulation of Spontaneously Contracting Cardiac Muscle Cells." *Biophysical Journal* 75.4 (1998): 2004–2014. Print.
- Carafoli, E. "The Role of Mitochondria in the Contraction-Relaxation Cycle and Other Ca^{2+} -Dependent Activities of Heart Cells." *Recent Adv. Stud. Cardiac. Struct. Metab.* 5 (1975) 151-163.
- Collins, Y., et al. "Mitochondrial Redox Signalling at a Glance." *Journal of Cell Science*, vol. 125, no. 7, Jan. 2012, pp. 1837–1837., doi:10.1242/jcs.110486.
- Duchen, Michael R. "Mitochondria and Calcium: From Cell Signalling to Cell Death." *The Journal of Physiology* 529.Pt 1 (2000): 57–68. PMC. Web. 20 Mar. 2018.
- Griffiths, Elinor J., and Guy A. Rutter. "Mitochondrial Calcium as a Key Regulator of Mitochondrial ATP Production in Mammalian Cells." *Biochimica Et Biophysica Acta (BBA) - Bioenergetics*, vol. 1787, no. 11, 2009, pp. 1324–1333., doi:10.1016/j.bbabi.2009.01.019.
- Kirichok, Yuriy, et al. "The Mitochondrial Calcium Uniporter Is a Highly Selective Ion Channel." *Nature*, vol. 427, no. 6972, 2004, pp. 360–364., doi:10.1038/nature02246.
- Lambert, David G., and Richard D. Rainbow. *Calcium Signaling Protocols*. Humana Press, 2013.
- Muller, Florian L., et al. "Trends in Oxidative Aging Theories." *Free Radical Biology and Medicine*, vol. 43, no. 4, 2007, pp. 477–503., doi:10.1016/j.freeradbiomed.2007.03.034.
- Perry, Seth W. et al. "Mitochondrial Membrane Potential Probes and the Proton Gradient: A Practical Usage Guide." *BioTechniques* 50.2 (2011): 98–115. PMC. Web. 20 Mar. 2018.
- Shadel, Gerald S., and Tamas L. Horvath. "Mitochondrial ROS Signaling in Organismal Homeostasis." *Cell*, vol. 163, no. 3, 2015, pp. 560–569., doi:10.1016/j.cell.2015.10.001.
- Zhang, X., and F. Gao. "Imaging Mitochondrial Reactive Oxygen Species with Fluorescent Probes: Current Applications and Challenges." *Free Radical Research*, vol. 49, no. 4, 2015, pp. 374–382., doi:10.3109/10715762.2015.1014813.

A Superior Direct Method for the Quantitative Analysis of DNA Fragments in Late-Stage Apoptosis

Multicellular organisms are made up of highly organized community of cells. For this community to thrive, it is important to establish homeostasis through complex cellular processes such as cell proliferation and apoptosis. The inappropriate shift in favor of either process has been implicated to cause disease. For instance, an increase in apoptotic activity in neurons is the source of various neurodegenerative disorders such as Alzheimer's and Parkinson's disease. In contrast, the loss of apoptotic mechanisms can lead to excessive cellular growth which is an underlying mechanism of how cells become cancerous. Overall, the role of apoptosis in disease is of high interest in scientific research.

Apoptosis

Apoptosis is a pathway of sophisticated and well-orchestrated programmed cell death. This cell-autonomous process is characterized by several distinct morphological and biochemical markers including cell and nuclear shrinkage, chromatin condensation, cytoplasmic membrane blebbing, and nuclear DNA fragmentation. These morphological changes all stem from two apoptotic pathways: the extrinsic or the intrinsic pathway. The extrinsic pathway is a receptor-mediated pathway activated by extracellular death receptor ligands (e.g. tumor necrosis factor (TNF) or Fas ligand (FasL)). The intrinsic pathway is induced intracellularly by environmental stressors resulting in mitochondrial membrane permeabilization and the release of apoptosis inducing factor (AIF) and

cytochrome c. Signals from both pathways are propagated through the caspase cascade, which ultimately lead to the downstream digestion of nuclear DNA by caspase activated nucleases. These features of apoptosis allow for the ability to use DNA fragmentation assays as the ultimate determinate for identifying apoptosis.

Apoptotic Assays Detecting DNA Fragmentation

There are various techniques for the assessment and identification of apoptotic DNA fragmentation. The earliest assay is a gel-based DNA laddering assay which involved using agarose gel electrophoresis to visualize and separate DNA fragments. Apoptotic DNA fragmentation is indicated by a distinctive 'ladder' like pattern of nucleosomal fragments approximately 180-200 base pairs in length. Although effective at generating qualitative data, this technique is not easily adaptable for high throughput use.

Another method of detection employs a double-antibody sandwich ELSIA assay consisting of anti-DNA and anti-histone antibodies to visualize DNA fragmentation during apoptosis. Although this assay is significantly more sensitive at detecting apoptotic DNA fragments and amenable for high-throughput uses (e.g. compound screening), it is labor intensive and the use of antibodies is costly.

TUNEL Assay

In 1992, Gorczyca et al. 1992 introduced a new method of measuring apoptotic DNA fragmentation utilizing terminal deoxynucleotidyl transferase (TdT) and nick translation or TUNEL assay. TdT catalyzes the addition of a fluorophore-labeled deoxyuridine triphosphate (dUTP) to the 3'-hydroxyl termini of a DNA double strand break (DSB).

Since the introduction of the TUNEL assay, it has become a widely-accepted in situ technique for identifying apoptotic cell death. Compared to previous methods, the TUNEL assay is more sensitive with the capacity to give a broad range of quantitative measurements over several orders of magnitude. Over the years, the TUNEL technique has been adapted and optimized for chromogenic and fluorogenic detection methods. Chromogenic TUNEL assays utilize

Parameters of Apoptosis

1. Loss of membrane asymmetry
2. Activation of pro-apoptotic Bcl-2 proteins
3. Caspase activation
4. Loss of mitochondrial membrane potential & release of cytochrome c.
5. Increase in Sub G1 population
6. Nuclear condensation
7. DNA fragmentation
8. Cell membrane blebbing

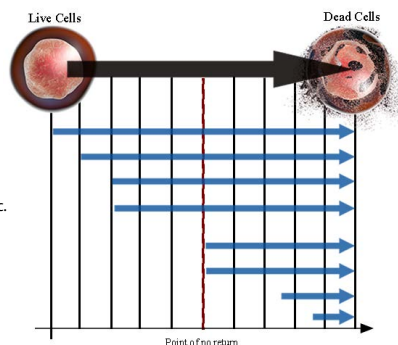


Figure 3.1. Outlines all of the parameters involved in apoptosis. It is important to note that these events do not occur in order. Many of them will overlap and will often occur simultaneously. Events 1 through 4 are biochemical features of apoptosis which do not necessarily end in cell death. Downstream apoptotic events 5 through 8 are strong indicators that a cell has committed to apoptosis, after which it is very unlikely the cell will survive.

dUTP conjugated to biotin and an enzyme-labeled streptavidin for high sensitive staining. The fluorogenic detection method relies on fluorescent dye-conjugated dUTP which is used for direct detection of DNA fragmentation.

Several variables influence the staining kinetics of TUNEL assays. Some of these variables include reagent concentration, fixation of sample, and accessibility of DNA strand breaks, which may vary between tissue or cell sample types. Therefore, standardizing your chosen TUNEL assay and having appropriate controls are critical in data collection and interpretation.

Cell Meter™ TUNEL Apoptosis Assay

AAT Bioquest's Cell Meter™ TUNEL Apoptosis Assay is optimized for fluorogenic detection and is available in either green or red fluorescence emission colors. AAT Bioquest's Cell Meter™ Assays include all the essential components and a robust protocol to detect and quantitate apoptotic DNA fragmentation in cells. Measuring apoptotic DNA fragments is achieved by catalytically incorporating a fluorescent dye modified deoxyuridine 5'-triphosphate nucleotide, Tunnelyte™ Green or Tunnelyte™ Red, to the 3' OH ends of DNA using TdT. Labeled DNA fragments can then be quantitated by flow cytometry or directly visualized by fluorescence microscopy.

Tunnelyte™ Green's peak absorption at 497 nm is well-suited for efficient excitation by instruments equipped with the 488 nm line of an argon-ion laser. Tunnelyte™ Red's peak absorption at 547 nm is efficiently excited with instruments using the helium-neon laser. For emission filter selection, Tunnelyte™ Green or Tunnelyte™ Red

can be read using a FITC (530/30) or Cy5 (660/40) filter, respectively. Because Tunnelyte™ nucleotides are amply separated from the blue spectrum, stains such as DAPI, Hoechst or Nuclear Violet™ LCS1 are suitable for live cell counterstaining in multicolor fluorescence applications.

Our Cell Meter™ TUNEL Apoptosis assay offers a distinct advantage over other commercially available TUNEL assays, because our kits

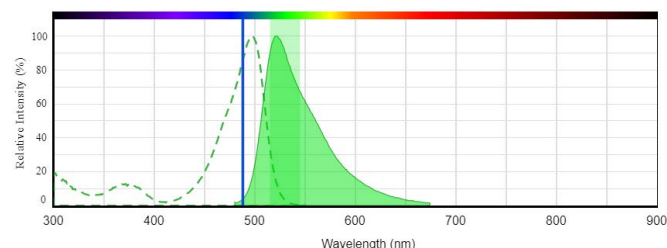


Image courtesy AAT Bioquest, Inc. (<https://www.aatbio.com>)

Figure 3.2. Absorption and emission spectrum for Tunnelyte™ Green. Excitation is at 488 nm (Blue laser line). Tunnelyte™ Green read with emission filter FITC (Green band).

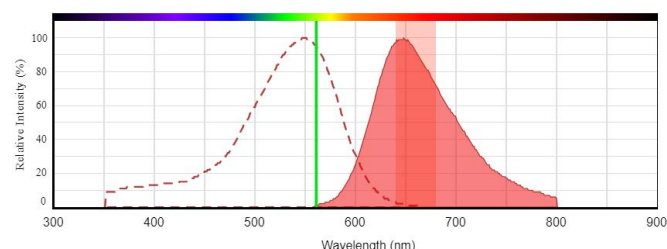


Image courtesy AAT Bioquest, Inc. (<https://www.aatbio.com>)

Figure 3.3. Absorption and emission spectrum of Tunnelyte™ Red. Excitation is at 561 nm (Green laser line). Tunnelyte™ Red read with emission filter Cy5 (Red band).

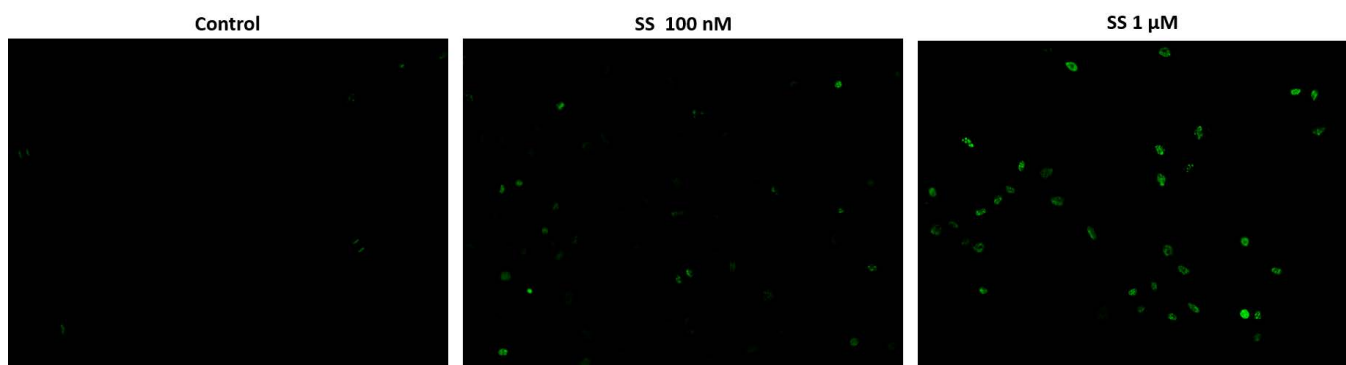


Figure 3.4. Fluorescence images of TUNEL reaction in HeLa cells treated with a chemical that induces apoptosis, staurosporin (SS). The HeLa cells are treated with 100 nM or 1 μM SS for 4 hours as compared to the untreated control. Cells were incubated with reaction mixture for 1 hour at 37 °C. The green fluorescence signal was analyzed using fluorescence microscope with a FITC filter set. Fluorescently labeled DNA strand breaks shows intense fluorescent staining in SS treated cells.

do not contain sodium or potassium cacodylate in the reaction buffer. Elimination of sodium cacodylate has a two-fold benefit. First, it is much safer to handle. Second, it provides a more sensitive and accurate apoptosis assay. Sodium cacodylate is a carcinogenic arsenic derivative that is highly toxic by ingestion, inhalation or skin contact. Because of the toxicity, it can induce apoptosis which inevitably leads to noise when measuring apoptosis in the assay.

The average market price and unit size of commercially available TUNEL assays is \$529 for 45 tests. AAT Bioquest's Cell Meter™ TUNEL assays offer the best value with each kit priced at \$295 and a unit size of 50 tests.

Conclusion

AAT Bioquest's Cell Meter™ TUNEL assay kits offers a simple, safe, and sensitive approach for detecting apoptotic DNA fragmentation. The direct incorporation of fluorescent nucleotides cuts down on assay time by reducing the number required incubation steps which allows for a quicker labeling of fragmented DNA. Finally our reagents are free of sodium cacodylate which results in the easier handling and disposal of the waste generated with our TUNEL assay.

References

1. Darzynkiewicz, Z., et al. "Features of Apoptotic Cells Measured by Flow Cytometry." *Cytometry*, vol. 13, no. 8, 1992, pp. 795–808., doi:10.1002/cyto.990130802.

2. Darzynkiewicz, Zbigniew, et al. "Analysis of apoptosis by cytometry using TUNEL assay." *Methods*, vol. 44, no. 3, 2008, pp. 250–254., doi:10.1016/j.ymeth.2007.11.008.
3. Kerr, J F R, et al. "Apoptosis: A Basic Biological Phenomenon with Wideranging Implications in Tissue Kinetics." *British Journal of Cancer*, vol. 26, no. 4, 1972, pp. 239–257., doi:10.1038/bjc.1972.33.
4. Liu, Xuesong, et al. "DFF, a Heterodimeric Protein That Functions Downstream of Caspase-3 to Trigger DNA Fragmentation during Apoptosis." *Cell*, vol. 89, no. 2, 1997, pp. 175–184., doi:10.1016/s0092-8674(00)80197-x.
5. Lu, Z., et al. "Nucleoplasmin regulates chromatin condensation during apoptosis." *Proceedings of the National Academy of Sciences*, vol. 102, no. 8, July 2005, pp. 2778–2783., doi:10.1073/pnas.0405374102.
6. Tang, Damu, and Vincent J. Kidd. "Cleavage of DFF-45/ICAD by Multiple Caspases Is Essential for Its Function during Apoptosis." *Journal of Biological Chemistry*, vol. 273, no. 44, 1998, pp. 28549–28552., doi:10.1074/jbc.273.44.28549.

Table 1. Price Comparison of TUNEL Assays

Company	Product Name	Unit Size	Price
AAT Bioquest	Cell Meter™ TUNEL Apoptosis Assay	50 tests	\$295
ThermoFisher	Click-iT™ TUNEL Alexa Fluor™ 488 Imaging Assay	1 kit (50 coverslips)	\$860
Promega	DeadEnd™ Fluorometric TUNEL System	60 reactions	\$597
Abcam	TUNEL Assay Kit – In situ BrdU-RED DNA Fragmentation	60 tests	\$735

Table 2. Cell Meter™ TUNEL Assays

Cat#	Product Name	Unit Size	Excitation (nm)	Emission (nm)
22849	Cell Meter™ TUNEL Apoptosis Assay *Green Fluorescence*	50 tests	497	520
22844	Cell Meter™ TUNEL Apoptosis Assay *Red Fluorescence*	50 tests	556	579

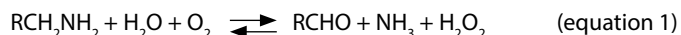
An Introduction to Lysyl Oxidase and Its Quantification

The improper regulation of lysyl oxidase (LOX) has been associated with several fibrotic diseases in humans. Elevated, or overregulated, levels of LOX activity have been linked with the pathogenesis of conditions such as pulmonary fibrosis, systemic sclerosis and liver cirrhosis. On the other hand, downregulation of LOX activity has been found in the development of aortic diseases such as aortic aneurysms and bone diseases such as osteolathyrism. More recently, LOX has been the focus of study due to its potential role in the metastasis of various cancers. For example, recent studies in mouse models have shown that LOX is a mediator for the metastasis of human breast cancer cells.

Because of its importance in biological processes, and its role in the pathogenesis of various human conditions, it is critical for research that there be specific and sensitive methods to quantify LOX activity. Here, two methods are reviewed: a radiometric method using tritium and a fluorimetric method using Amplite™ Red.

Overview

Lysyl oxidase belongs to a family of enzymes known as amine oxidases. This family of enzymes catalyzes the oxidation of amines to aldehydes. A generic form of this reaction is shown below:



An important thing to note is the byproduct of amine oxidation, which is a molecule of hydrogen peroxide. This is important because the production of hydrogen peroxide can be coupled to an enzymatic reaction, such as H_2O_2 -dependent HRP, to monitor LOX activity.

In organisms, amine oxidases are used to regulate the levels of many biologically important amines. For example, histamine, the well-known molecule involved in local immune responses, is broken down by the amine oxidase, diamine oxidase (DAO). In the case of LOX, the oxidation target is the amine group on lysine side chains.

Synthesis and Activity

In cells, lysyl oxidase is typically first synthesized as a 50 kDa protein

precursor called prolysyl oxidase. This inactive form of the protein is then glycosylated in the Golgi Complex, forming an N-glycosylated proenzyme. After glycosylation, it is transported via vesicles to the cell membrane, wherein it is secreted into the extracellular matrix (ECM). While not fully established, evidence suggests that it is during this secretion into the ECM that LOX becomes activated. In particular, studies have pointed to cell surface peptidases as the enzymes which cleave the prolysyl oxidase peptide into the catalytically active, 32 kDa lysyl oxidase form.

In terms of activity, lysyl oxidase requires two cofactors to function: copper and lysyl tyrosyl quinone (LTQ). As with many copper amine oxidases (CAO), the bound copper, Cu(II), serves to spontaneously generate the quinone cofactor, creating a redox active site in the enzyme. For LOX, the quinone cofactor is LTQ, which is formed through the crosslinking of a tyrosine residue and a lysyl side chain.

Functionally, lysyl oxidase is involved in the crosslinking of collagen or elastin in the extracellular matrix. The formation of crosslinks between collagen fibers, or elastin fibers, by LOX typically occurs in a two-step process. First, LOX catalyzes the oxidative deamination of lysyl residues on tropocollagen and tropoelastin. This reaction produces peptidyl α -amino adipic- δ -semialdehyde, which is also called allysine. In the second step, the produced aldehyde intermediary, allysine, undergoes a spontaneous condensation reaction. This reaction results in the crosslinking of collagen, or elastin, lysyl sidechains. In collagen, crosslinking occurs between three lysine residues, forming pyridinoline (also known as hydroxylysyl pyridinoline). In elastin, crosslinking occurs between four lysine residues, forming desmosine.

Cancer Metastasis

As discussed previously, lysyl oxidase is functionally important in collagen, or elastin, crosslinking. As such, it can also be inferred that LOX plays an important role in the structural integrity and remodeling of the extracellular matrix, of which collagen and elastin are critical compounds. This is supported by studies of various human fibrotic diseases, in which LOX is improperly regulated. But perhaps what is not as apparent is the role of LOX in the metastasis of tumors and cancer cells. And yet, several well-conducted studies on human

breast cancer cell lines demonstrate why such may be the case. That is, why LOX activity may be central to the metastasis of cancer cells.

A study conducted by Dawn et al. compared the expression of LOX (and lysyl oxidase-like enzymes LOXL, LOXL2, LOXL3 and LOXL4) in two different human breast cancer cell lines. One was MDA-MB-231, a highly invasive/metastatic cell line, while the other was MCF-7, a poorly invasive/nonmetastatic cell line. What the research group found was that LOX and LOXL2 activity was strongly associated with the invasive MDA-MB-231 cell line while none of the LOX or LOXL proteins were highly expressed in the poorly invasive MCF-7 cell line. Blocking LOX expression with an antisense oligonucleotide or inhibiting LOX activity with an irreversible inhibitor, β -aminopropionitrile, also decreased invasive activity in the MDA-MB-231 cell line.¹⁴ These results were replicated in and supported by a plethora of studies since.

A paper by Cox et al. proposes a theory for why LOX activity may be so closely tied to tumor metastasis. The theory is that LOX activity, whether normal expression or overexpression, creates a fibrotic milieu that enhances tumor colonization and outgrowth of tumor cells. That is, LOX activity creates a scaffold upon which tumor cells can spread. This idea garners further support from studies which show that inhibition of LOX does not inhibit primary tumor growth, but does restrict secondary (i.e. metastatic) tumor activity. In a biological context, this theory is very logical as it is, in principle, the same concept as soft tissue wound healing, wherein myofibroblasts deposit fibers such as collagen to promote the division and spread of epithelial and endothelial cells over an injury site.

Tritium Release End Point Assay

One of the first, and perhaps still the most sensitive, lysyl oxidase activity assays is the tritium release end point assay. Here, end point assay simply refers to a single quantification after a specified incubation period, as opposed to a kinetic assay, which quantifies activity at several instances over a duration of time. With the tritium release end point assay, the sample of interest (i.e. a tissue or organ culture) is first incubated in a lysine-deficient medium, followed by a medium with tritium-labeled lysine in the presence of β -aminopropionitrile (BAPN). This promotes the exhaustion of endogenous, non-labeled

lysine and allows for pulse labeling with tritium-labeled lysine. After a specified incubation period, the sample of interest is lysed and the tritium containing solution is collected by vacuum distillation. Quantification of the tritiated water ($[^3\text{H}]\text{OH}$) yields measurements proportional to LOX activity. This assay works on the principle that LOX-catalyzed oxidative deamination of lysine residues releases tritium into solution at a one to one rate (see equation 1).

The tritium release end point assay is the most sensitive assay for LOX activity because it is a direct measurement of the oxidative deamination product, that is, tritiated water. However, it has three big disadvantages. First, it is very inconvenient and labor intensive to conduct, requiring vacuum distillation of each sample. This makes it an impractical method for medium to large scale testing. Second, it requires the use of radioactive isotopes. While not dangerous through external exposure, ingestion, inhalation or absorption through the skin can pose a radioactive hazard. Third, and finally, special equipment is required to conduct radioactive counting of the tritiated water, which may not be available to many researchers. Because of these disadvantages, a spectroscopic method for monitoring LOX activity should be strongly considered.

Amplite™ Fluorimetric Lysyl Oxidase Activity Assay

An example of a spectroscopic LOX assay is the Amplite™ Fluorimetric Lysyl Oxidase Assay Kit (AmLOX™). It uses a HRP enzyme-coupled assay system with Amplite™ Red as the HRP substrate. It also includes a proprietary LOX substrate that closely mimics endogenous LOX substrates like collagen and elastin. This allows for much more accurate and representative measurements of LOX activity. Spectroscopic methods can be used to monitor lysyl oxidase by coupling its activity with a reporter enzyme. Typically, horseradish peroxidase (HRP) is chosen. This is because of two reasons. First, HRP is well-studied and readily available, in part due to its popularity in ELISAs. Second, HRP is well situated to take advantage of the oxidative deamination reaction of LOX. HRP requires hydrogen peroxide, a byproduct in the LOX mechanism, as the oxidizing agent in its own redox reaction. This forms a tight coupling between LOX activity and HRP activity, with hydrogen peroxide being the limiting reagent. Finally, all that is needed is a spectroscopically active (chromogenic or fluorogenic) substrate for the HRP, which can then be monitored using spec-

troscopic instrumentation, such as plate readers. One of the early HRP substrates used to monitor LOX activity was homovanillic acid, however better alternatives have since been developed, such as TMB and Amplite™ Red.

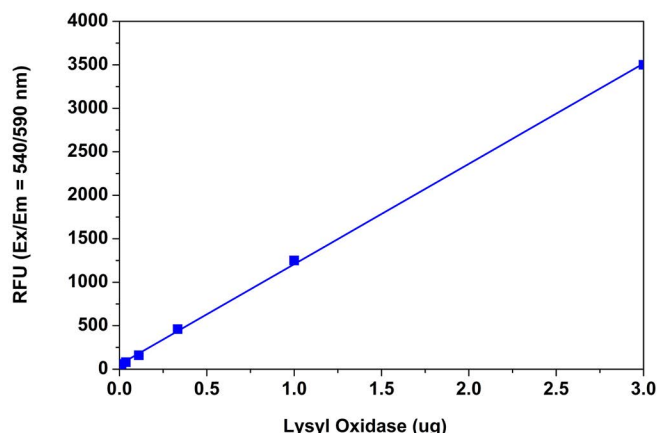


Figure 4.1. Lysyl oxidase dose response was measured on a solid black 96-well with Amplite™ Fluorimetric Lysyl Oxidase Assay Kit (Cat# 15255) using a Gemini fluorescence microplate reader (Molecular Devices). As low as 40 ng/mL of lysyl oxidase can be detected with 30 minutes incubation (n=3).

One important thing to note is that, in principle, spectroscopic assays, such as AmLOX™, will be less sensitive than tritium release end point assays. This is because spectroscopic assays are indirect measurement methods which utilize a secondary detection system (i.e. H₂O₂-dependent HRP) whereas the tritium release end point assay is a direct measurement method that quantifies the byproduct of the LOX reaction. Thus, in theory, AmLOX™ will not achieve the same sensitivity as tritium-based assay. In practice, however, AmLOX™ shows comparable results to tritium release end point assays. Our testing has shown that AmLOX™ is able to detect sub-ng/well of lysyl oxidase, a detection limit which more than satisfies the requirement for most applications.

AmLOX™ demonstrates comparable experimental sensitivity to tritium release end point assays. But AmLOX™ has several other

distinct features that make it a better overall assay choice than tritium-based ones. First, AmLOX™ does not use any radioactive or highly toxic chemicals. Second, AmLOX™ can be paired with very standard microplate instrumentation found in many labs. Elaborating on this point, AmLOX™ can actually be read in two different modes. It can be used as a colorimetric assay in conjunction with an absorbance microplate (read at 576 nm). It can also be used as a fluorimetric assay and paired with a fluorescence microplate reader (using 540 nm as the excitation and 590 nm as the emission). This offers researchers extra flexibility in terms of experimental design. Finally, unlike tritium-based assays, there is no laborious vacuum distillation required. This assay can be completely and conveniently executed in a standard 96- or 384- well microplate.

A sample protocol has been provided below:

1. Prepare sample in microplate beforehand
2. Add 50 µL of AmLOX™ working solution into each well
3. Incubate at 37 °C for 10 to 30 minutes, protected from light
4. Read fluorescence using a fluorescence microplate reader (using Ex = 540 nm and Em = 590 nm)

References

1. Aumiller, V., Strobel, B., Romeike, M., Schuler, M., Stierstorfer, B. E., & Kreuz, S. (2017). Comparative analysis of lysyl oxidase (like) family members in pulmonary fibrosis. *Scientific reports*, 7(1), 149.
2. Cox, T. R., Gartland, A., & Erler, J. T. (2016). Lysyl oxidase, a targetable secreted molecule involved in cancer metastasis. *Cancer research*, 76(2), 188-192.
3. Mecham, R. (2018) *Methods in Extracellular Matrix Biology*. Retrieved from <https://books.google.com>
4. Rucker, R. B., Kosonen, T., Clegg, M. S., Mitchell, A. E., Rucker, B. R., Uriu-Hare, J. Y., & Keen, C. L. (1998). Copper, lysyl oxidase, and extracellular matrix protein cross-linking. *The American journal of clinical nutrition*, 67(5), 996S-1002S.

Table 1. Nucleic Acid Staining Reagents and Assay Kits

Cat #	Product Name	Size	Ex (nm)	Em (nm)
15255	Amplite™ Fluorimetric Lysyl Oxidase Assay Kit *Red Fluorescence*	500 tests	571	585
13512	Amplite™ MMP-3 Activity Assay Kit *Green Fluorescence*	100 tests	498	520
13510	Amplite™ Universal Fluorimetric MMP Activity Assay Kit *Green Fluorescence*	100 tests	494	521
13511	Amplite™ Universal Fluorimetric MMP Activity Assay Kit *Red Fluorescence*	100 tests	545	576

Fluorescent Phalloidin: A Practical Stain for Visualizing Actin Filaments

Actin is a highly conserved family of proteins that form microfilaments. Its amino acid sequence varies less than 20% between organisms as simple as yeast to higher eukaryotes such as humans. Due to its intracellular abundance in eukaryotic cells, well within micromolar concentrations, actin participates in the most protein-protein interactions than any other known protein. It possesses a unique ability to dynamically polymerize into filamentous actin (F-actin) from its monomeric state. Interactions between F-actin and regulatory proteins such as actin-binding proteins rapidly assemble and disassemble actin filaments organizing them into actin bundles and cytoskeletal networks. These higher-order structures provide the mechanical and structural support essential for a multitude of cellular processes including intracellular transport, cytokinesis, cell motility, polarity and cell shape, gene regulation and signal transduction. Because actin is essential in so many biological processes, tools (actin-specific antibody and phalloidin derived stains) for the visualization of these actin structures are essential in research.

Actin-Specific Antibodies: The Earliest F-Actin Stains

The earliest actin staining technique adopted an immunohistochemical (IHC) approach by employing fluorophore labeled antibodies to stain against actin microfilaments (Lazarides and Weber, 1974). Although this approach functionally works for actin visualization, it did have disadvantages.

First, immunostaining is labor intensive. It requires careful consideration of parameters including antibody selection, fixation, antigen-retrieval, and blocking. If the desired antibody is not commercially available, then additional time and cost is needed to develop and purify the appropriate antibodies.

Second, the utilization of an antibody may be an obstacle. Antibodies, which are generally large in size (~150 kDa), are impermeable to cell membranes and require fixation and permeabilization of the cell prior to actin staining. Proper fixation is critical, and is dependent on epitope sensitivity and the antibody being used. Fixation preserves cell structures but it can reduce the antigenicity of certain cellular

compartments. Therefore, it is imperative to optimize fixation conditions because under or over-fixation can drastically reduce or prohibit tissue immunoreactivity.

Lastly, the non-specific binding of antibody conjugates to both monomeric and polymeric actin generates high levels of background noise which results in low resolution stains. To combat such limitations, novel actin-binding components with enhanced specificity for F-actin were developed as suitable alternatives, the most notable being phalloidin.

Phalloidin

Phalloidin, the main representative of the phallotoxin family, is a bicyclic heptapeptide isolated from the poisonous death cap mushroom, *Amanita phalloides*. It possesses a high binding affinity for the grooves between F-actin subunits over monomeric G-actin. Once bound to F-actin, phalloidin shifts the equilibrium of monomers and filaments toward the filaments position, and inhibits ATP-hydrolysis. The interaction stabilizes actin filaments by preventing subunit dissociation, and it promotes actin polymerization by lowering the critical concentration. As a consequence, these characteristics have made phalloidin derivatives useful stains in visualizing F-actin and cytoskeletal networks.

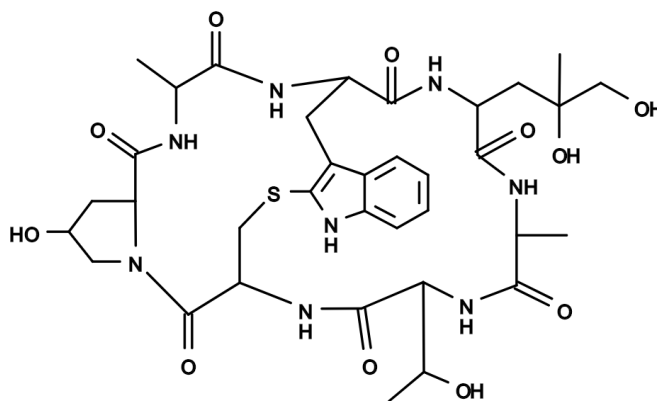


Figure 5.1. The chemical structure for Phalloidin *CAS#: 17466-45-4*(Cat# 5301).

Properties of Phalloidin Derivatives

Since its initial use to stain actin in the late 1970s, phalloidin and its fluorescent derivatives remain the gold standard for visualizing cellular actin filaments. Compared to IHC staining, phalloidin derivatives offer significant advantages for labeling actin. They provide a convenient method for identifying, labeling, and quantitating F-actin formation in fixed and permeabilized cells and tissue sections.

Phalloidin derivatives are water soluble and when used at nanomolar concentrations can selectively stain F-actin. Unlike some antibodies against actin, phalloidin's capacity to bind more tightly to actin filaments over monomers decreases non-specific staining and background noise which produce high contrast between stained and unstained areas. In comparison to antibodies, phalloidin derivatives are small (<2 kDa) and phalloidin bound filaments do not impede functional properties of the filaments. The small size also permits for denser F-actin labeling producing more detailed stains when imaged at higher resolutions. In addition, because actin is evolutionarily conserved, the binding properties of phalloidin derivatives can be utilized in staining a wide range of animal and plant cells.

Choosing the Right Phalloidin Derivative

Due to its notable staining abilities, an array of phalloidin derivatives has been developed to study and visualize actin filaments and actin-related structures. Summaries of the properties of unlabeled, biotinylated, and fluorescently labeled phalloidin derivatives can be found below.

Unlabeled Phalloidin

Unlabeled phalloidin has limited uses. Other than serving as promoter of actin polymerization, unlabeled phalloidin is typically used as a control in blocking F-actin staining.

Biotinylated Phalloidin

Biotinylated phalloidin provides an indirect method for visualizing and quantitating actin filaments. It requires the use of a fluorescent or enzyme-conjugated avidin or streptavidin for visualization. Whilst indirect detection offers the benefit of signal amplification, the need for additional reagents increases costs and assay time. Additionally,

when staining with biotinylated phalloidin a higher concentration of the phalloidin conjugate is required, approximately two-fold more than needed with fluorescent phalloidin. Regardless of the inconveniences, biotinylated phalloidin are favorable for pull-down and immunoprecipitation assays for investigating protein interactions and colocalization with F-actin.

Fluorescent Phalloidin-iFluor™ Conjugates

Exploiting the excellent fluorescence properties of our iFluor™ dyes, AAT Bioquest has developed a series of phalloidin conjugates spanning the full color spectrum which selectively bind to F-actins. Used at nanomolar concentration, these iFluor™ phalloidin derivatives are convenient for many actin-related assays. Such assays include labeling, identifying, and quantitating F-actins in formaldehyde-fixed and permeabilized tissue sections, cell-cultures, or cell-free experiments. Compared to traditional fluorescein isothiocyanate (FITC) and rhodamine conjugates, Phalloidin-iFluor™ conjugates offer F-actin stains that are superior in brightness and photostability. Phalloidin-iFluor™ conjugates are equivalent, and in most cases superior, to Alexa Fluor® conjugates in performance. Finally, Phalloidin-iFluor™ conjugates are more affordable as they are available in a unit size of 300 tests for \$145 versus Alexa Fluor®'s \$433 price tag.

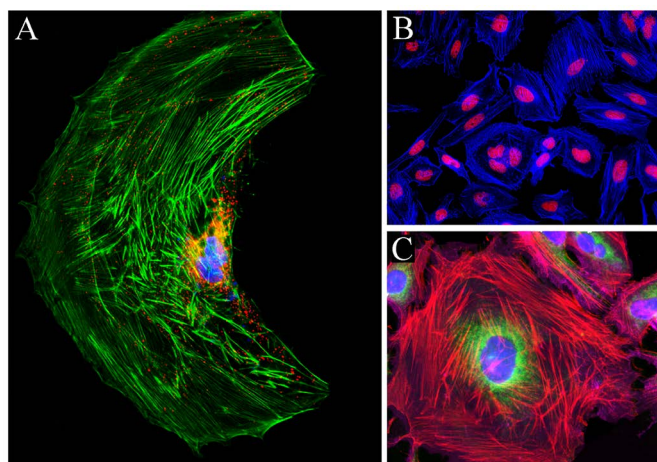


Figure 5.2. A) CPA cell labeled with F-actin stain Phalloidin iFluor™ 488 (Cat#231115, Green), and co-stained with lysosome dye LysoBrite™ Red (Cat#22658) and nuclei stain Nuclear Blue™ DCS1 (Cat#17548). B) HeLa cells labeled with F-actin stain Phalloidin-iFluor™ 350 (Cat#23110, Blue) and co-stained with nuclei stain Nuclear Red™ DCS1 (Cat#17552, Red). C) HeLa cells labeled with F-actin stain Phalloidin-iFluor™ 555 (Cat#23119, Red). Co-stained with mitochondria stain MitoLite™ Green FM (Cat#22695, Green), nuclei stain Nuclear Blue™ DCS1 (Cat#17548, Blue) and plasma membrane stain Cellpaint™ Deep Red (Cat#22681, Magenta).

We encourage the research community to try our Phalloidin-iFluor™ conjugates with their respective protocols for a more intense fluorescence in their F-actin staining. Phalloidin-iFluor™ 700, iFluor™-750 and iFluor™-790 conjugates are among the few near-infrared stains available with sufficient spectral separation from commonly used red fluorophores

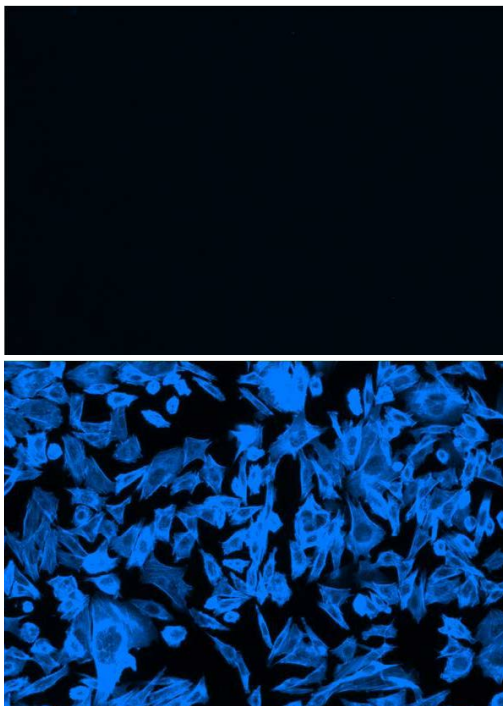


Figure 5.3. Fluorescence images of HeLa cells fixed with 4% formaldehyde then stained with Cell Navigator™ F-Actin Labeling Kit *Blue Fluorescence* (Cat#22660) in a Costar black 96-well plate. Cells were labeled with iFluor™ 350-Phalloidin (Blue, Cat#23110) with (Top) or without (Bottom) pre-treatment of phalloidin for 10 minutes.

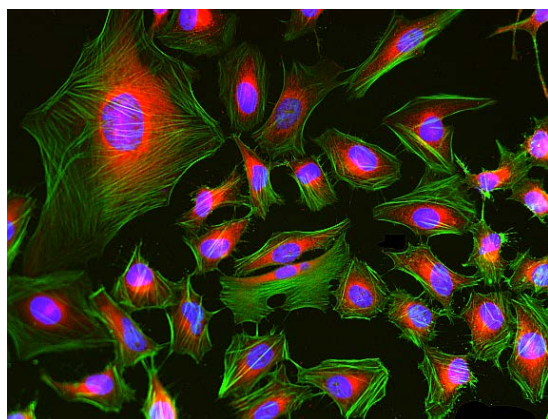


Figure 5.4. Fluorescence image of HeLa cells stained with Phalloidin-iFluor™ 488 Conjugate (Green, Cat#23115) using fluorescence microscope with a FITC filter set (Green). The cells were fixed in 4% formaldehyde, co-labeled with mitochondrial dye MitoLite™ Red FX600 (Red, Cat#22677) and Nuclear Blue™ DCS1 (Blue, Cat#17548).

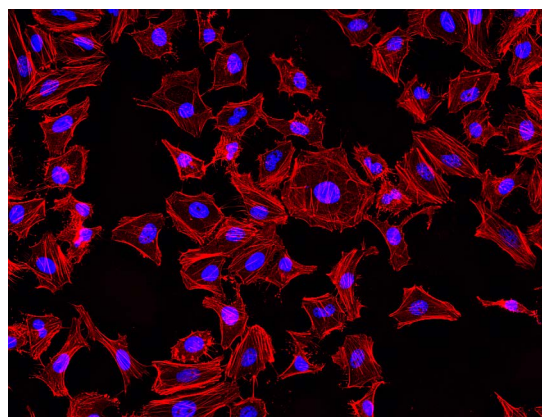


Figure 5.5. Fluorescence image of HeLa cells stained with Phalloidin-iFluor™ 514 (Cat#23116) Conjugate using fluorescence microscope with a TRITC filter set (Red). Fixed cells were counterstained with Nuclear Blue™ DCS1 (Blue, Cat#17548).

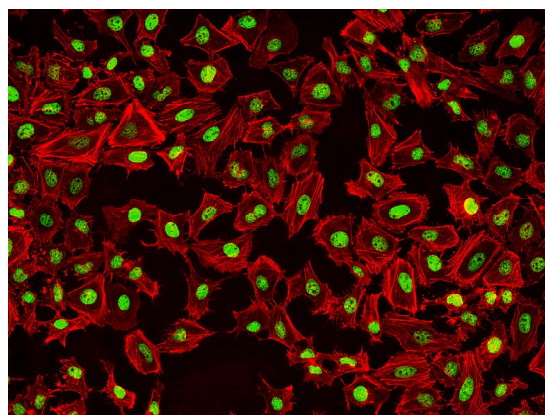


Figure 5.6. Fluorescence image of HeLa cells stained with Phalloidin-iFluor™ 532 Conjugate (Cat#23117) using fluorescence microscope with a TRITC filter set (Red). Fixed cells were counterstained with Nuclear Green™ DCS1 (Green, Cat#17550).

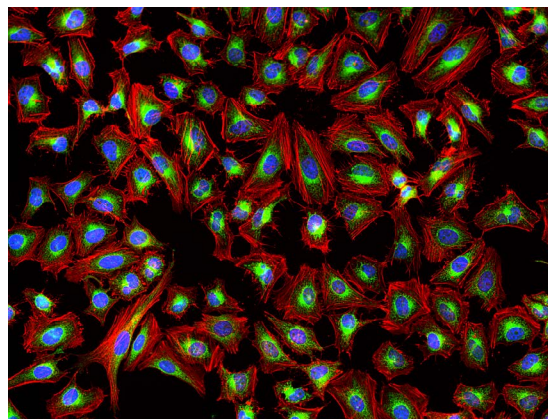


Figure 5.7. Fluorescence image of HeLa cells stained with Phalloidin-iFluor™ 647 Conjugate (Red, Cat#23127) using fluorescence microscope with a Cy5 filter set (Red). Live cells were first stained with mitochondrial dye MitoLite™ Green (Green, Cat#22675). After fixation in 4% formaldehyde, cells were labeled with Phalloidin-iFluor™ 647 and counterstained with Nuclear Blue™ DCS1 (Blue, Cat#17548).

Staining F-actin with Phalloidin-iFluor™ Conjugates

The protocol below outlines in detail a method for F-actin staining of cultured cells utilizing AAT Bioquest's Phalloidin-iFluor™ 488 conjugate (Cat# 23115).

Storage and Handling Conditions

It is important to note that phalloidin is toxic, although the contents present in each vial are potentially lethal to a mosquito (LD_{50} of phalloidin = 2 mg/kg), it should always be handled with care.

Phalloidin-iFluor™ 350 to iFluor 596 conjugates come packaged as 1000X stock solution in DMSO and are ready to be used as supplied. Phalloidin-iFluor™ 633 to iFluor™ 790 conjugates come packaged as a lyophilized powder and must be prepared in 1000X stock solution. Both conjugates are stable for at least six months when stored at proper conditions. If not to be used immediately, store Phalloidin-iFluor™ conjugate at -20 °C, protect from light and avoid freeze-thaw cycles.

Required Reagents

- Phalloidin-iFluor™ 488 conjugate
- PBS
- 3.0 - 4.0% Methanol-free formaldehyde
- 0.1% Triton X-100
- BSA
- Cell culture or tissue sample for staining
- (Optional) ethanolamine
- (Optional) FluoroQuest Mounting Medium with DAPI

1X Phalloidin-iFluor™ 488 Conjugate Working Solution

1. Prepare working solution by adding 1 μ L of 1000X Phalloidin-iFluor 488 conjugate DMSO solution to 1 mL of PBS with 1% BSA.
2. Mix well by pipetting solution up and down. This makes enough staining solution for 10 wells at 100 μ L/well.
3. Aliquot any unused 1000X Phalloidin-iFluor 488 DMSO stock solution and store in proper conditions.

Note: Staining may vary between different cell types. For optimal performance, the concentration of phalloidin conjugate working solution should be prepared accordingly.

Staining Procedure for Cultured Cells

Note: If using paraffin-embedded tissue samples, a deparaffinization and re-hydration step is required. For a deparaffinization and re-hydration protocol see Appendix.

1. Fix cells in 3.0 – 4.0% methanol-free formaldehyde in PBS at room temperature for 10 to 30 minutes.
2. Aspirate fixation solution carefully.
3. Rinse cells 2 to 3 times in PBS
4. (Optional) Quench excess formaldehyde with 10 mM ethanolamine in PBS for 5 minutes.
5. Increase permeability by adding 0.1% Triton X-100 in PBS into fixed cells for 3 to 5 minutes.
6. Rinse the cells 2 to 3 times in PBS.
7. In a 96-well plate, add 100 μ L/well of Phalloidin-iFluor 488 conjugate working solution into the fixed cells.
8. Stain the cells at room temperature for 20 to 90 minutes.
9. Rinse cells gently 2 to 3 times with PBS to remove excess phalloidin conjugate.
10. (Optional) Add a small drop of FluoroQuest Mounting Medium with DAPI and incubate for 2 hours. This inhibits photobleaching and counterstain nucleus with DAPI.
11. Observe cells by using a fluorescence microscope fitted with the appropriate filter. iFluor 488 excitation and emission is 493 nm and 517 nm, respectively.

Appendix

Deparaffinization and Re-Hydration of Paraffin-Embedded Tissue Slides:

A deparaffinization step is only required when using paraffin-embedded tissue sections. Prior to F-actin staining, it is important to de-paraffinize and rehydrate your tissue slides. Incomplete removal of paraffin will result in poorly or non-stained sections.

Materials and Reagents

- Xylene
- 100% ethanol
- 95% ethanol
- 70% ethanol
- 50% ethanol

Method

1. Heat tissues slides at 55 °C for 10 minutes to melt paraffin.
2. Deparaffinize tissue slides in 2 changes of xylene or xylene substitute for 5 minutes each.
3. Gradually hydrate tissue slides by transferring slides through 100%, 95% and 70% alcohol for 5 minutes each.
4. Inhibit endogenous peroxidase activity by incubating tissue slides in 3% H₂O₂ for 10 minutes each.
5. Rinse in PBS 2X for 5 minutes each.
6. Proceed with F-actin staining protocol.

References

1. Dominguez, Roberto, and Kenneth C. Holmes. "Actin Structure and Function." Annual review of biophysics 40 (2011): 169–186. PMC. Web. 19 Mar. 2018.
2. Firat-Karalar, Elif Nur, and Matthew D. Welch. "New Mechanisms and Functions of Actin Nucleation." Current opinion in cell biology 23.1 (2011): 4–13. PMC. Web. 19 Mar. 2018.
3. Lazarides, Elias, and Klaus Weber. "Actin Antibody: The Specific Visualization of Actin Filaments in Non-Muscle Cells." Proceedings of the National Academy of Sciences of the United States of America 71.6 (1974): 2268–2272. Print.
4. Lengsfeld, Anneliese M. et al. "Interaction of Phalloidin with Actin." Proceedings of the National Academy of Sciences of the United States of America 71.7 (1974): 2803–2807. Print.
5. Melak, Michael, et al. "Actin Visualization at a Glance." Development, vol. 144, no. 4, 2017, doi:10.1242/dev.150052.
6. Wulf, E et al. "Fluorescent Phalloidin, a Tool for the Visualization of Cellular Actin." Proceedings of the National Academy of Sciences of the United States of America 76.9 (1979): 4498–4502. Print.

Tabel 1. Nucleic Acid Staining Reagents and Assay Kits

Cat #	Product Name	Size	Ex (nm)	Em (nm)
22660	Cell Navigator™ F-Actin Labeling Kit *Blue Fluorescence*	500 tests	353	442
22661	Cell Navigator™ F-Actin Labeling Kit *Green Fluorescence*	500 tests	498	520
22663	Cell Navigator™ F-Actin Labeling Kit *Orange Fluorescence*	500 tests	546	575
22664	Cell Navigator™ F-Actin Labeling Kit *Red Fluorescence*	500 tests	583	603
23100	Phalloidin-AMCA Conjugate	300 tests	353	442
23103	Phalloidin-California Red Conjugate	300 tests	583	605
23101	Phalloidin-Fluorescein Conjugate	300 tests	492	518
23110	Phalloidin-iFluor™ 350 Conjugate	300 tests	353	442
23111	Phalloidin-iFluor™ 350 Conjugate	300 tests	400	421
23115	Phalloidin-iFluor™ 350 Conjugate	300 tests	493	517
23116	Phalloidin-iFluor™ 350 Conjugate	300 tests	520	547
23117	Phalloidin-iFluor™ 350 Conjugate	300 tests	542	558
23119	Phalloidin-iFluor™ 350 Conjugate	300 tests	556	574
23122	Phalloidin-iFluor™ 350 Conjugate	300 tests	590	618
23125	Phalloidin-iFluor™ 350 Conjugate	300 tests	634	649
23127	Phalloidin-iFluor™ 350 Conjugate	300 tests	650	665
23128	Phalloidin-iFluor™ 350 Conjugate	300 tests	681	698
23129	Phalloidin-iFluor™ 350 Conjugate	300 tests	692	708
23130	Phalloidin-iFluor™ 350 Conjugate	300 tests	752	778
23131	Phalloidin-iFluor™ 350 Conjugate	300 tests	787	808
23102	Phalloidin-Tetramethylrhodamine Conjugate	300 tests	546	575

International Distributors

Australia:

Assay Matrix Pty Ltd.
Email: info@assaymatrix.com
Website: <http://www.assaymatrix.com>

Jomar Life Research
Email: info@liferesearch.com
Website: <http://www.liferesearch.com>

Austria:

Biomol GmbH
Email: info@biomol.de
Website: <http://www.biomol.de>

Belgium:

Gentaur BVBA
Email: info@gentaur.com
Website: <http://www.gentaur.com>

Canada:

Cedarlane Laboratories Ltd.
Email: sales@cedarlanelabs.com
Website: <http://www.cedarlanelabs.com>

China:

Tianjin Biolite Biotech Co., Ltd
Email: info@tjbiolite.com
Website: <http://www.tjbiolite.com>

Croatia:

Biomol GmbH
Email: info@biomol.de
Website: <http://www.biomol.de>

Czech Republic:

Scintila, s.r.o.
Email: rejtharkova@scintila.cz
Website: <http://www.scintila.cz>

Denmark:

Nordic BioSite ApS
Email: info@nordicbiosite.dk
Website: <http://www.nordicbiosite.dk>

Estonia:

Biomol GmbH
Email: info@biomol.de
Website: <http://www.biomol.de>

Nordic BioSite AB
Email: info@biosite.se
Website: <http://www.biosite.se>

Finland:

Nordic BioSite OY
Email: info@biosite.fi
Website: <http://www.biosite.fi>

France:

EUROMEDEX
Email: research@euromedex.com
Website: <http://www.euromedex.com>

Interchim
Email: interchim@interchim.com
Website: <http://www.interchim.com>

Germany:

Biomol GmbH
Email: info@biomol.de
Website: <http://www.biomol.de>

Hong Kong:

Mai Bio Co., Ltd
Email: info@maibio.com
Website: <http://www.maibio.com>

Hungary:

IZINTA Trading Co., Ltd.
Email: baloghk@izinta.hu
Website: <http://www.izinta.hu>

Iceland:

Nordic BioSite AB
Email: info@biosite.se
Website: <http://www.biosite.se>

India:

Biochem Life Sciences
Email: info@bcls.in
Website: <http://www.bcls.in>

GenxBio Health Sciences Pvt. Ltd,
Email: sales@genxbio.com
Email: genxbio@gmail.com
Website: <http://www.genxbio.com>

Ireland:

Stratech Scientific Ltd.
Email: info@stratech.co.uk
Website: <http://www.stratech.co.uk>

Israel:

ADVANSYS Technologies for Life Ltd.
Email: info@advansys.co.il
Website: <http://www.advansys.co.il>

Italy:

Space Import Export S.r.l.
Email: info@spacesrl.com
Website: <http://www.spacesrl.com>

Valter Occhiena S.r.l.
Email: vo@valterocchiena.com
Website: <http://www.valterocchiena.com>

Japan:

Cosmo Bio Co., Ltd.
Email: mail@cosmobio.co.jp
Website: <http://www.cosmobio.co.jp>

Nacalai Tesque, Inc.
Email: info@nacalaiusa.com
Website: <http://www.nacalai.com>

Wako Pure Chemical Industries, Ltd.
Email: labchem-tec@wako-chem.co.jp
Website: <http://www.wako-chem.co.jp>

Korea:

Cheong Myung Science Corporation
Email: cms@cmscorp.co.kr
Website: <http://www.cmscorp.co.kr>

Kimnfriends Corporation
Email: kimnfriends@hanmail.net
Website: <http://www.kimnfriends.co.kr>

Latvia and Lithuania:

Nordic BioSite AB
Email: info@biosite.se
Website: <http://www.biosite.se>

Netherlands:

ITK Diagnostics BV
Email: info@itk.nl
Website: <http://www.itk.nl>

Norway:

Nordic BioSite AB
Email: info@biosite.se
Website: <http://www.biosite.se>

Poland and Slovenia:

Biomol GmbH
Email: info@biomol.de
Website: <http://www.biomol.de>

Romania:

SC VitroBioChem SRL
Email: office@vitro.ro
Website: <http://www.vitro.ro>

Singapore and Other South Asian Countries:

Axil Scientific Pte Ltd.
Email: info@axilscientific.com
Website: <http://www.axilscientific.com>

Slovakia:

Scintila, s.r.o.
Email: rejtharkova@scintila.cz
Website: <http://www.scintila.cz>

South American Countries and Regions:

Impex Comércio Internacional Ltda.
Email: impexcom@terra.com.br
Website: <http://www.impexbrasil.com.br>

Spain and Portugal:

Deltaclon S. L
Email: info@deltaclon.com
Website: <http://www.deltaclon.com>

Sweden:

Nordic BioSite AB
Email: info@biosite.se
Website: <http://www.biosite.se>

Switzerland:

LuBioScience GmbH
Email: info@lubio.ch
Website: <http://www.lubio.ch>

Taiwan:

Cold Spring Biotech Corp.
Email: csbiotech@csbiotech.com.tw
Website: <http://www.csbiotech.com.tw>

Rainbow Biotechnology Co., LTD.
Email: rainbow@rainbowbiotech.com.tw
Website: <http://www.rainbowbiotech.com.tw>

Turkey:

Suarge Biyoteknoloji Ltd. Co.
Email: info@suarage.com
Website: <http://www.suarage.com/en/>

United Kingdom:

Stratech Scientific Ltd.
Email: info@stratech.co.uk
Website: <http://www.stratech.co.uk>